Proceedings of the Estonian Academy of Sciences,
201?, ??, ?, ??–??
https://doi.org/10.3176/proc.201?.?.??
Available online at www.eap.ee/proceedings

Coupling with adjustable torsional stiffness

First Author[a], Second Author[b*], Third Author[b], ...

[a] First author's affiliation and full address
[b] Second and third authors' affiliation and full address

Received ?? Month 20??, accepted ?? Month 20??, available online ?? Month 20??

Abstract. Torsional vibration problems occur regularly in large machinery. The torsional natural frequencies of a rotating system can typically be found with torsional analysis but predicting if resonance or torsional vibrations will appear is often more difficult. Taking all possible sources of torsional vibration excitation into account can be challenging; torsional vibration problems may appear unexpectedly due to unknown excitation frequencies in the system. In this study a coupling with adjustable torsional stiffness is presented. Since the torsional stiffness of the coupling can be adjusted it potentially be used to tune the torsional natural frequencies rotating systems. The coupling design presented in this study provides clear benefits compared to typical flexible couplings. For In typical flexible couplings with elastomeric elements, the torsional can be adjusted by changing the elastomers. However, this often requires disassembly of the coupling, and the torsional stiffness adjustment has to be done in large increments. In the presented coupling design, the torsional stiffness can be adjusted without disassembly. The torsional stiffness can be tuned to a wide range of stiffnesses and with arbitrarily small increments if necessary. In this study, the torsional stiffness of the coupling was determined with analytical calculations, FEM simulation and experimentally. In the experimental tests, the torsional stiffness range of the coupling was measured to be between 8–126 kNm/rad. The coupling design was considered to be successful, since the study confirmed that the torsional stiffness of the coupling can be adjusted to a wide range of different values. Experimental measurements confirm the calculated and simulated stiffness values.

Key words: Coupling, Torsional Stiffness, Torsional Vibrations, Adjustable, Stiffness, Resonance.

1. INTRODUCTION

Torsional vibrations are present in almost every rotating system and some machines are inherently prone to torsional vibrations. For example, pumps and combustion engines produce torsional vibrations due to their operating principles. Torsional vibrations produce cyclic stresses, which can make the machine elements susceptible to fatigue damage [1]. The vibrations can manifest heavily due to resonance if the excitation frequency of the system coincides with torsional natural frequencies of the system. Excitation frequencies present in a system can be difficult to predict beforehand and problems caused by torsional vibrations can appear unexpectedly [2]. Unexpected vibration problems may cause severe damages to machines. Adjusting the torsional natural frequency of a system can reduce the vibrations caused by the resonance.

The torsional stiffness of a coupling affects the torsional natural frequencies in rotating systems. It needs to be considered especially in applications where torsional vibration problems are known to frequently occur. However, usually the torsional stiffness of a coupling is not easily adjustable. In commercial couplings

* Corresponding author, his/her e-mail address

flexible element couplings, the adjusting of the torsional stiffness typically requires disassembly of coupling and changing of the flexible elements. If torsional vibration problems caused by resonance manifest unexpectedly, for example in the first runs of the machine, disassembling the coupling and adjusting the stiffness may require a significant amount of work. In the worst case, large components need to be removed, reassembled and realigned to adjust the torsional stiffness of the coupling.

In this study, a coupling design with adjustable torsional stiffness is presented. The adjustment of the torsional stiffness is based on changing the effective length of a shaft and cantilever beams in the coupling. Easily adjustable torsional stiffness is a benefit for large machines and for other rotating systems where the torsional behaviour or properties are difficult to calculate or predict accurately beforehand. Various prototypes of couplings and joints with adjustable torsional stiffness similar to the coupling presented in this study have been developed previously [3–10]. These designs use a wide range of different methods to adjust the torsional stiffness such as springs, beams, magnetorheological fluids and elastomers, and pneumatics.

The main goal of this study was present a novel adjustable stiffness coupling design and to determine the torsional stiffness range and feasibility of the design. The torsional stiffness of the coupling was determined by using analytical calculations, FEM simulations and with experimental measurements. The static measurements were done using a lathe as a test bench. The output half coupling was fixed to the lathe tailstock. The input half was clamped to the lathe chuck to allow only rotation around the torsional axis. Torque was applied to the input half with torque wrench. The torque and the angular displacement were measured. From the torque and the angular displacement, the torsional stiffness of the coupling was calculated. With some modifications and with suitable dimensioning the coupling design could potentially be applied to industrial applications to prevent torsional vibration problems.

2. COUPLING DESIGN WITH ADJUSTABLE TORSIONAL STIFFNESS

Fig. 1 presents the coupling and the main parts. The coupling consists of input and output halves at the its ends, 6 beams, adjustable flange and middle shaft. The shaft of the torque source is attached to the input half. Torque is transferred from the input half through the beams to the adjustable flange. The flange transfers the torque to the middle shaft by a spline. The middle shaft is splined and it is fixed to the output half. The torsional stiffness of the coupling is determined by the effective lengths of the beams and the middle shaft, and they are adjusted by moving the adjustable flange longitudinally. The effective lengths of the beams and the shaft are roughly inverse. Thus, when the beams are at their stiffest position, the shaft stiffness is at its lowest and vice versa. Both the beams and the middle shaft have high stiffnesses when their effective lengths are low. However, the lowest stiffness of the middle shaft is much higher than the lowest stiffness of the beams, so the highest stiffness is achieved when the adjustable flange is near the input half.

The beams were made of high strength low alloy steel. High strength steel can prevent possible yielding of the beams if the coupling is loaded heavily when the effective length of the beams is high. 3D printed PLA plastic parts were placed between the beams and their grooves to allow for the possibility to easily change the thickness of the beams by 3D printing new plastic fitting parts for beams with a different thickness. Also, in the adjustable flange the plastic parts allow the flange to slide efficiently when it is moved. The beams are slightly larger than the groove in the plastic parts, so there is no clearance which could cause problems during operation. The beams are attached to the input half with screws and to the output half with sliding connection. The sliding connection allows the beam to move in longitudinal direction but restricts the beam from coming out from its groove.

The shape of the beams has a significant impact to the stiffness of the coupling. The beams can be designed to be for example tapered or wider at certain position. Changing the shape of the beams can be used to adjust the behaviour and the stiffness characteristics of the coupling. In the presented design, the shape of the beams is rectangular to test the shape which is as simple as possible.

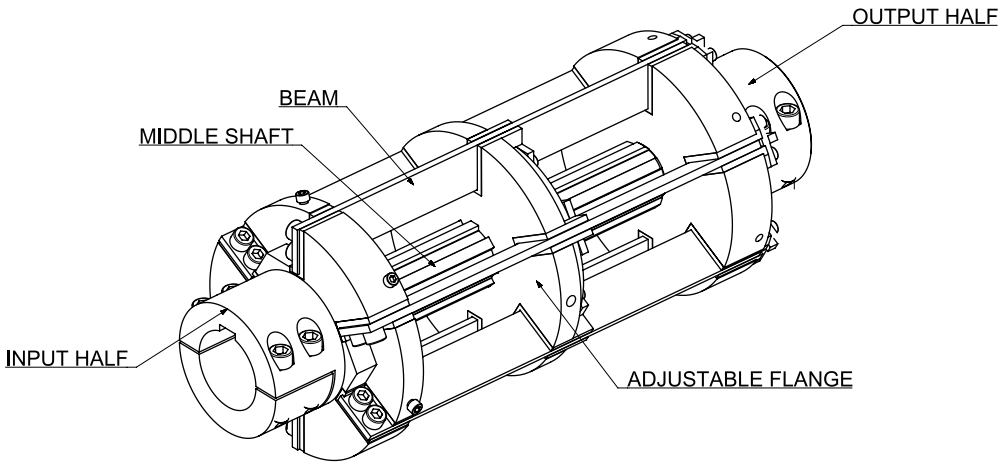

Fig. 1: The main parts of the coupling

3. METHODS

The torsional stiffness of the coupling design (with different operation points i.e. effective lengths of the beams and the shaft) was determined in three ways: analytical calculations, FEM simulations and experimental measurements.

3.1. Analytical calculations

The analytical calculations of the torsional stiffness were done by calculating the effect of the stiffness of the beams and the middle shaft. The splined middle shaft was simplified to a plain round shaft with a suitable thickness (diameter at the bottom of the splines). The total torsional stiffness of the coupling was calculated by considering the beams and the shaft in series.The geometrical and material parameters are presented in Table 1 and the dimensions used in the calculations are presented in Fig. 2.

Table 1: Geometrical and material parameters used in the analytical calculations.

Parameter & unit	Radius r [mm]	Young's modulus E [GPa]	Shear modulus G [GPa]	Beam thickness b [mm]	Beam height h [mm]	Shaft diameter d [mm]
Value	78.5	209	78	6	40	46

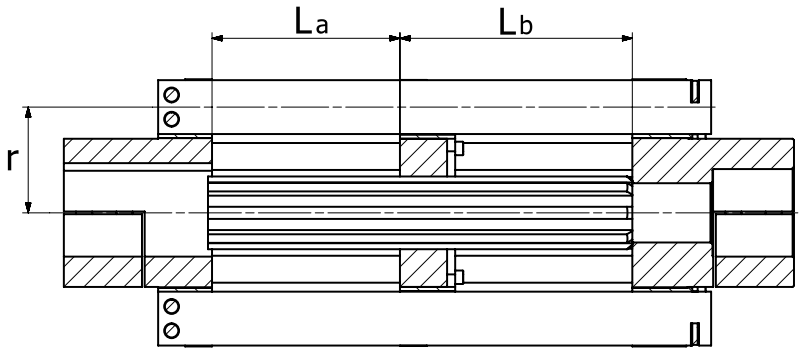

Fig. 2: Dimensions used in the calculations

The total torsional stiffness of the coupling was calculated by combining the total stiffness of the beams and the torsional stiffness of the middle shaft. When torque is applied to the coupling, the beams are subjected to bending and twisting. The stiffness of the beams was calculated by combining the stiffness caused by both types of displacement. The formula for springs in series was used in the calculation. The beam stiffness is multiplied by 6, which is the number of beams in the coupling.

When torque is applied to the coupling, the beams are subjected to bending and twisting. The stiffness of the beams was calculated by combining the stiffness caused by both types of displacement. The beam stiffness versus bending was calculated using basic torsional stiffness formula

$$k_{bending} = \frac{Fr}{\theta} \tag{1}$$

where $k_{bending}$ is the beam stiffness against bending, Fr is torque, and θ is the angle of twist. The angle of twist was calculated by applying the basic cantilever beam deflection. The beams were treated to be fixed on one end and free on the other and the load to be applied to the free end of the beam. The angle of twist was defined as

$$\theta = \frac{\delta}{r} \tag{2}$$

where δ is deflection of the beam, which is defined as

$$\delta = \frac{FL_a^3}{3EI} \tag{3}$$

where L_a is the effective length of the beams and E is the Young's modulus of the beams. I is the second moment of inertia defined as

$$I = \frac{hb^3}{12} \tag{4}$$

where h is the height, and b is the thickness of the beam. Thus, the total stiffness against bending is

$$k_{bending} = \frac{3EIr^2}{L_a^3} \tag{5}$$

The beams also twist torsionally when the torque is applied to the coupling. The beam stiffness against torsional twisting is calculated with equation

$$k_{twisting} = \frac{GJ_a}{L_a} \tag{6}$$

J_a is the torsion constant for rectangular cross-section. J_a is defined as

$$J_a = \beta hb^3 \tag{7}$$

where β is 0.3, which is defined by the height to width ratio of the cross-section[11]. The stiffness of the middle shaft k_s was defined in accordance with the torsional rigidity definition. For simplicity, the shaft is treated as a plain round shaft in the calculations.

$$k_{shaft} = \frac{GI_p}{L_b} \tag{8}$$

L_b is the effective length of the middle shaft. I_p is the torsion constant for circular cross-section, which is defined as

$$I_p = \frac{\pi d^4}{32} \tag{9}$$

The total torsional stiffness of the coupling was calculated by combining the total stiffness of the beams and the stiffness of the middle shaft. The calculation was done with the formula for springs in series. The total beam stiffness is multiplied by 6, which is the number of beams in the coupling.

$$k = \left(\frac{1}{6(k_{bending} + k_{twisting})} + \frac{1}{k_{shaft}}\right)^{-1} \tag{10}$$

3.2. Simulated torsional stiffness

The torsional stiffness was also determined using FEM (Finite Element Method) simulations. The simulations were done using Siemens NX with basic static solver. Before the simulations, the 3D-model of the coupling was pre-processed to simplify the simulation. Excess parts and detailed geometry like fillets, screws and the spline tooth were removed. The coupling was meshed with tetrahedral elements. The element size was 3 mm for the beams and the plastic parts. Larger 6 mm mesh was used in all other parts. The boundary conditions are presented in Fig. 3. The bore surface of the output half was fixed with all 6 degrees of freedom constrained. A torque load was applied to the bore surface of the input half.

The output half, the middle shaft and the adjustable flange were rigidly connected. The plastic parts between the beams and the grooves were considered to be rigidly connected to their grooves. Also, the beams were rigidly connected to the plastic parts from the area around of the screws in the input half side. Non-linear contact was applied between other areas where the beams and the plastic parts are touching. Since contacts do not provide boundary conditions to the simulation, springs with very small stiffness were added to the output ends of the beams. The springs act as a boundary condition for the beams and to the input half of the coupling.

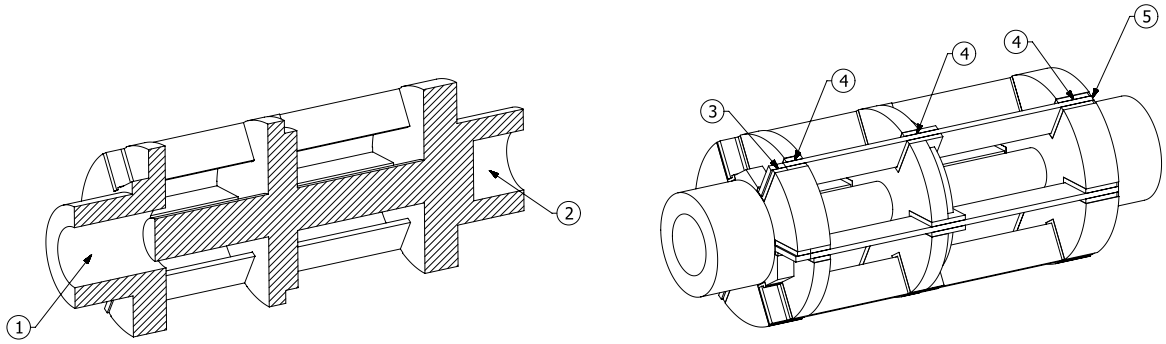

Fig. 3: Forces and boundary conditions in the simplified coupling. 1. Torque load, 2. Fixed constraint, 3. Rigid connection, 4. Non-linear contact, 5. Springs with small stiffness.

3.3. Static torsional stiffness measurement

The coupling was tested experimentally with static torsional stiffness test. The coupling was fixed except the rotation of the input half. Torque was applied to the input half and the angular displacement was measured. From the torque and angular displacement, the torsional stiffness was calculated. The goal of this test was to validate the coupling design and to determine the torsional stiffness range of the coupling.

A lathe was used as a test bed for the torsional stiffness test. The test setup is presented in Fig. 4. The coupling was mounted between the tailstock and the lathe chuck. The output half of the coupling was fixed with the tailstock. A special tool was made to properly mount the output half to the tailstock. The input half of the coupling was clamped to the lathe chuck, which allowed only rotation around the torsional axis of the coupling. Thus, the test bed fixed every degree of freedom in the output half and the input half was left with only the torsional rotation free.

The torque was applied to the input half of the coupling using a digital torque wrench. The torque wrench was clamped to the center bore of the input half. Weights were used to apply a constant force to the torque wrench. The weights were hanged from the handle of the torque wrench and the amount of torque applied to the input half was measured with the torque wrench.

The applied torque caused an angular displacement in the input half. The angular displacement of the input half was measured using a Heidenhain MT-12 linear displacement sensor. Another displacement sensor was mounted to the fixed output half to confirm that it does not rotate or move during the measurements. The sensors were attached to a dial indicator stand. To measure the angular displacement in the input half the spindle of the sensor was set against the surface of a beam in the input half of the coupling. The spindle of the sensor was set as perpendicular as possible against the measured surface to prevent cosine error. As the chuck rotated the measured surface moved the spindle of the displacement sensor. Since the sensor measures only linear displacement, it was converted to angular displacement by dividing the linear displacement with the distance from the axis of rotation to the point of measurement. Measuring the angular displacement indirectly with this method produces an error, since the point that is measured is moving in an arc and not linearly. However, the measured angular displacements were small, so the effect of the error was considered negligible.

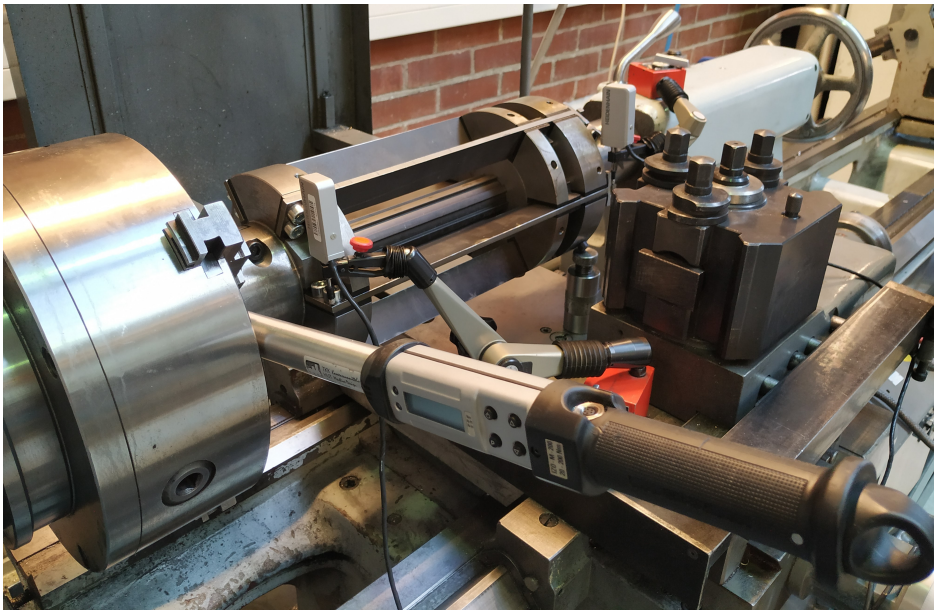

Fig. 4: The coupling in the test bench. The input half is attached to the lathe chuck which allows rotation in torsional direction. The output half is fixed by attaching it to the lathe tailstock. Two displacements sensor are mounted to measure the displacement of the input end and to ensure that the fixed output end does not rotate. The torque is applied by placing weights to the torque wrench.

Next, the measurement procedure is presented.

1. The adjustable flange was moved as close as possible to input half, which is the position with highest torsional stiffness.
2. Torque was applied by adding the weight on the torque wrench.
3. The torque and the angular displacement were measured. After the measurements, the weights were removed.
4. The torque and displacement were measured total of 5 times at the current adjustable flange position and the results were averaged to derive a value of the torsional stiffness.
5. The adjustable flange was moved.
6. Steps 2-5 were repeated until the whole stiffness range of the coupling was measured.

4. RESULTS

The static torsional stiffness of the coupling was determined with analytical calculations, FEM simulation and practical experiments. The results were obtained for the whole range of possible adjustable flange positions. The range is 0-260 mm measured from the input half. The comparison of determined torsional stiffness can be seen as function of the adjustable flange position in fig. 5. Only moderate deviations can be noticed from the determined stiffness curves when they are compared to each other. The simulated and measured stiffness have very similar type of curve, which confirms that the FEM simulation corresponds to the actual coupling with good accuracy.

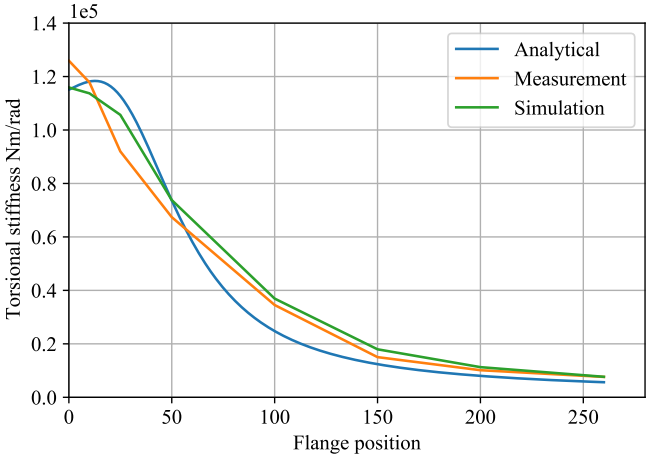

Fig. 5: Torsional stiffness curves from analytical calculations, FEM simulations and practical experiment. The stiffness values are plotted as a function of adjustable flange position.

5. DISCUSSION

The analytically calculated torsional stiffness curve has a different shape compared to the other curves, having a distinct peak (Fig. 6a). The shape of the stiffness curve is caused by the interaction between the beam stiffness and the shaft stiffness. When the adjustable flange position is 0 the effective length of the beams is at shortest and the effective length of the shaft is at its longest. The short effective length of the beams causes them to have really high stiffness compared to the shaft. Since the beams and the shaft are in series, with low flange position the stiffness of the coupling is determined almost fully by the stiffness of the shaft. As the flange position is increased the stiffness of the beams start to decrease rapidly as their effective length increases. When the flange position is at around 13mm the stiffness of the beams has decreased enough so total stiffness of the coupling peaks and starts to decrease. The stiffness of the beams decreases rapidly until the flange position reaches around 70 mm. The rapid decrease of the beam stiffness decreases the total stiffness of the coupling substantially. After the flange position is increased over to 100 mm, the beam stiffness has decreased enough so it determines almost fully the total torsional stiffness of the coupling.

The behaviour of the beams can be analysed in depth by dividing the beam stiffness to its components (Fig. 6b). As torque is applied to the coupling the beams bend and twist. The effect of bending stiffness and twisting stiffness were calculated and the total beam stiffness is their sum. Both stiffness values are high when the flange position is low. However, the bending stiffness is much higher and decreases more slowly than the twisting stiffness, which causes the bending stiffness to determine the total beam stiffness at low flange positions. At higher flange positions the bending stiffness decreases to very low values while the twisting stiffness stays higher. Thus, at higher flange positions the total beam stiffness is mostly determined by the twisting stiffness of the beams.

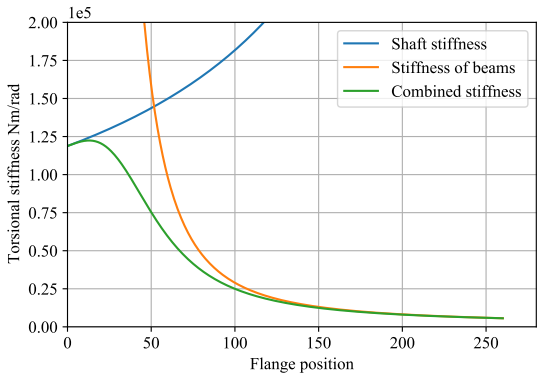

(a) Graph of the shaft stiffness, stiffness of the beams, and stiffness of the coupling. It presents how the stiffness of the shaft and the beams affect the stiffness of the coupling.

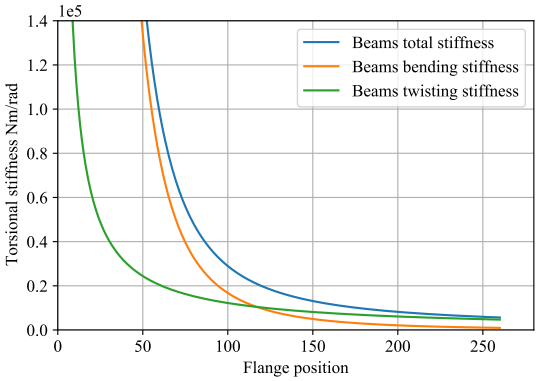

(b) Graph of the stiffness of the beams divided to stiffness against bending and against twisting. The graph demonstrates how the total stiffness of the beams is formed.

Fig. 6: Graphs demonstrating the formation of total torsional stiffness of the coupling.

Potential further research would be to test the dynamic properties of the coupling. The coupling could be attached to a rotating system and its capacity to change the torsional natural frequencies could be tested. It would confirm the coupling design to be usable for reducing critical torsional vibrations and its potential for research and industry applications.

In the current design the stiffness can be adjusted manually but the stiffness adjusting mechanism could be automated for example with a servo motor and linear guides. A servo motor would allow automated control of the torsional natural frequency of the rotating system. Thus the system could be applied to automatically reduce torsional vibrations by adjusting the torsional stiffness of the coupling.

6. CONCLUSION

In this study, a coupling with adjustable torsional stiffness was presented. The torsional stiffness is adjusted by changing the effective length of rectangular beams in the coupling. The torsional stiffness of the coupling was determined with analytical calculations, FEM simulation and experimental measurement. The measured stiffness of the coupling corresponds well with the analytical calculations and FEM simulation. The results of the experiment validated the coupling design as the torsional stiffness of the coupling was adjusted successfully to a wide range of stiffness values.

REFERENCES

1. Eshleman, R. Torsional vibration of machine systems. *NASA STI/Recon Technical Report A*, 1977, 13–22.
2. Corbo, M. and Malanoski, S. Practical design against torsional vibration. 1996, 189–222.
3. Urbansky, M., Kassay, P., and Vojtkova, J. New design solutions of tangential pneumatic torsional vibration tuners. *Scientific Journal of Silesian University of Technology. Series Transport*, 2019, **103**, 183–191.
4. Lee, K. H., Park, J. E., and Kim, Y. K. Design of a stiffness variable flexible coupling using magnetorheological elastomer for torsional vibration reduction. *Journal of Intelligent Material Systems and Structures*, 2019, **30**. https://doi.org/10.1177/1045389X19862378.
5. Wolf, S. and Hirzinger, G. A new variable stiffness design: matching requirements of the next robot generation. 2008.
6. Zheng, Y., Zhang, X., Luo, Y., Zhang, Y., and Xie, S. Analytical study of a quasi-zero stiffness coupling using a torsion magnetic spring with negative stiffness. *Mechanical Systems and Signal Processing*, 2018, **100**. https://doi.org/10.1016/j.ymssp.2017.07.028.
7. Choi, J., Hong, S., Lee, W., Kang, S., and Kim, M. A robot joint with variable stiffness using leaf springs. *IEEE Transactions on Robotics*, 2011, **27**. https://doi.org/10.1109/TRO.2010.2100450.
8. Li, Z., Chen, W., and Bai, S. A novel reconfigurable revolute joint with adjustable stiffness. Vol. 2019-5. 2019.
9. Gradu, M. and Schlernitzauer, T. L. (inventors). Stabilizer bar with variable torsional stiffness. patent US 7207574 B2.
10. Post, R. F. (inventor). Magnetic bearing element with adjustable stiffness. patent US 8581463 B2.
11. Ugural, A. and Fenster, S. *Advanced Strength and Applied Elasticity*. Pearson Education, 2003.